



Climate change impacts in the design of drainage systems: case study of Portugal

Article

Accepted Version

Modesto Gonzalez Pereira, M. G., Sanches Fernandes, L. F., Barros Macário, E. M., Gaspar, S. M. and Pinto, J. G. (2015) Climate change impacts in the design of drainage systems: case study of Portugal. *Journal of Irrigation and Drainage Engineering*, 141 (2). 05014009. ISSN 0733-9437 doi: [https://doi.org/10.1061/\(ASCE\)IR.1943-4774.0000788](https://doi.org/10.1061/(ASCE)IR.1943-4774.0000788) Available at <http://centaur.reading.ac.uk/37936/>

It is advisable to refer to the publisher's version if you intend to cite from the work.

Published version at: [http://dx.doi.org/10.1061/\(ASCE\)IR.1943-4774.0000788](http://dx.doi.org/10.1061/(ASCE)IR.1943-4774.0000788)

To link to this article DOI: [http://dx.doi.org/10.1061/\(ASCE\)IR.1943-4774.0000788](http://dx.doi.org/10.1061/(ASCE)IR.1943-4774.0000788)

Publisher: American Society of Civil Engineers

All outputs in CentAUR are protected by Intellectual Property Rights law, including copyright law. Copyright and IPR is retained by the creators or other copyright holders. Terms and conditions for use of this material are defined in the [End User Agreement](#).

www.reading.ac.uk/centaur

CentAUR

Central Archive at the University of Reading

Reading's research outputs online

1 **Climate change impacts in the design of drainage systems –**

2 **A case study for Portugal**

3
4 Mário Jorge Modesto Gonzalez Pereira¹; Luís Filipe Sanches Fernandes²;
5 Eduarda Maria Barros Macário³; Sónia Morgado Gaspar⁴; Joaquim Ginete
6 Pinto⁵

7
8 Final word version from:

9 Pereira MG, Sanches Fernandes LF, Macário E, Gaspar S, Pinto JG (2015) Impact of
10 Projected Climate Change in the Design of Urban Stormwater Drainage Systems – A
11 Case Study for Portugal. J. Irrig. Drain. Eng., 141, 05014009.
12 doi:10.1061/15(ASCE)IR.1943-4774.0000788

13
14
15

¹ Assistant Professor, Centre for the Research and Technology of Agro-Environmental and Biological Sciences, CITAB, University of Trás-os-Montes and Alto Douro, UTAD, Quinta de Prados, 5000-801 Vila Real, Portugal; and IDL, Faculdade de Ciências da Universidade de Lisboa, Campo Grande, Edifício C8, Piso 3, 1749-016 Lisboa, Portugal (corresponding author). E-mail: gpereira@utad.pt

² Assistant Professor, Centre for the Research and Technology of Agro-Environmental and Biological Sciences, CITAB, University of Trás-os-Montes and Alto Douro, UTAD, Quinta de Prados, 5000-801 Vila Real, Portugal; and Department of Engineering, University of Trás-os-Montes and Alto Douro, UTAD, Quinta de Prados, 5000-801 Vila Real, Portugal. E-mail: lfilipe@utad.pt

³ M.Sc. Graduate of Civil Engineering, Department of Engineering, University of Trás-os-Montes and Alto Douro, UTAD, Quinta de Prados, 5000-801 Vila Real, Portugal. E-mail: edu.mbmacario@gmail.com

⁴ M.Sc. Graduate of Civil Engineering, Department of Engineering, University of Trás-os-Montes and Alto Douro, UTAD, Quinta de Prados, 5000-801 Vila Real, Portugal. E-mail: snmorgado09@gmail.com

⁵ Associate Professor in Regional Climate and Synoptic Meteorology, Department of Meteorology, University of Reading, Whiteknights, PO Box 217, Reading, Berkshire, RG6 6AH, United Kingdom; and Institute for Geophysics and Meteorology, University of Cologne, Pohligstr. 3, D-50969 Köln, Germany. E-mail: j.g.pinto@reading.ac.uk; and jpinto@meteo.uni-koeln.de

16 **Abstract**

17 This study aims to assess the necessity of updating the Intensity-Duration-Frequency
18 (*IDF*) curves used in Portugal to design building storm-water drainage systems. A
19 comparative analysis of the design was performed for the three pre-defined rainfall
20 regions in Portugal using the *IDF* curves currently in use and estimated for future
21 decades. Data for recent and future climate conditions simulated by a global/regional
22 climate model chain (ECHAM5/MPI-OM1/COSMO-CLM) are used to estimate
23 possible changes of rainfall extremes and its implications for the drainage systems. The
24 methodology includes the disaggregation of precipitation up to sub-hourly scales, the
25 robust development of *IDF* curves and the correction of model bias. Obtained results
26 indicate that projected changes are largest for the plains in Southern Portugal (5 – 33%)
27 than for mountainous regions (3 – 9%) and that these trends are consistent with
28 projected changes in the long term 95th-percentile of the daily precipitation throughout
29 the 21st century. We conclude for the need to review the current precipitation regime
30 classification and change the new drainage systems towards larger dimensions to
31 mitigate the projected changes in extreme precipitation.

32

33 ASCE Subject Headings: Climate change, Hydraulic design, Drainage systems,
34 Precipitation, Portugal

35 Author keywords: *IDF* curves; Climate change; Drainage systems design; Extreme
36 precipitation.

37 **Introduction**

38 The recent IPCC Special Report on Managing the Risks of Extreme Events and
39 Disasters to Advance Climate Change Adaptation (IPCC 2012) have recently provided
40 evidence that the intensity of extreme precipitation may increase even in areas where
41 total precipitation decreases (Diodato et al. 2011; IPCC 2012). This implies shorter
42 return periods for extreme rainfall. In particular, the changes in the water cycle are
43 likely change the frequency and intensity of floods and droughts for many parts of the
44 world (IPCC 2012); hence, the knowledge of the regime of heavy precipitation in
45 regional terms both under recent and future climate conditions is critical (Beijo et al.
46 2005; IPCC 2012).

47 From the engineering point of view, empirical approaches are used to link extremes of
48 precipitation with physical structures. The Intensity-Duration-Frequency (*IDF*) curves
49 represent key information for the design of urban and building storm-water drainage
50 systems, as they provide maximum precipitation intensity related to a given length and a
51 given return period (Brandão et al. 2001). The *IDF* curves are mathematically described
52 by the power law behaviour dependence of the precipitation intensity (*I*) of the duration
53 (*t*),

54

$$I = a \times t^b \quad (1)$$

55

56 where *a* and *b* are the *IDF* parameters. In Portugal, the designers of building storm-
57 water drainage systems work according to the Portuguese law (DR 1995), which
58 stipulates the *IDF* curves developed by Matos and Silva (1986). However, long-term
59 trends in rainfall intensities and the projected climate change in terms of the water cycle
60 fosters the assessment of the impact of extreme precipitation in the current and future
61 design of building storm-water drainage systems and the possible update of *IDF* curves

62 (e.g. Fowler and Kilsby 2003 and Vasiljevic et al. 2012). Recently, the impact of
63 climate change on *IDF* curves have been assessed in several studies performed for the
64 U.S. and Canada (Mailhot et al. 2007; Peck et al. 2012; Zhu et al. 2012; Das et al. 2013;
65 Zhu 2013; Zhu et al. 2013). However, these studies did not assess the possible
66 consequences of such changes to the design of building storm-water drainage systems
67 as the one conducted in northern Europe, for the sewer system of Fredrikstad, Norway
68 by Nie et al. (2009).

69 Global circulation models (GCM) and regional climate models (RCM) are important
70 tools to study the impact of climate change on meteorological, chemical, hydrological
71 and hydraulic processes. Given pre-defined scenarios of the world development, these
72 models provide projections of different meteorological variables for possible future
73 conditions of the climate system (Meehl et al. 2007; Taylor et al. 2012). The GCMs
74 used for these climate projections have typically resolutions of 100-300 km, which is
75 typically too low for direct use of model output in regional studies. Downscaling
76 techniques, using RCMs, statistical downscaling or a combination of both have been
77 used to obtain results at a finer spatial and temporal time scale (e.g. Maraun et al. 2010).
78 Furthermore, model biases towards the real climate conditions must be adequately
79 assessed, interpreted and corrected before applications can be performed.

80 In the specific case of urban building drainage systems, the design requires knowledge
81 of rainfall depth intensity values over short periods of time (between minutes to hours).
82 On this assumption, it is necessary to use appropriate methodology capable of
83 performing the disaggregation of daily precipitation depth in sub-daily and sub-hourly
84 precipitation (e.g., Pui et al. 2012). A possible approach is the method of the fragments,
85 introduced by Svanidze in the 1960s (Svanidze 1964, Svanidze 1980), as it is a
86 commonly used method in the precipitation disaggregation (Sharif and Burn, 2007;

87 Arganis-Juárez et al. 2008) used to obtain the disaggregation coefficients presented in
88 Brandão et al. (2001), which is an official publication of the national Directorate of
89 Services of Water Resources with the results of the analysis of extreme precipitation in
90 Continental Portugal.

91 Several studies have assessed the impact of climate change on the design of drainage
92 systems, using model simulations/climate scenarios, with converging results in different
93 parts of the world towards increased precipitation intensity and the potential under-
94 designing of drainage systems (e.g. Nie et al 2009; Rosenberg et al. 2010; He et al.
95 2011; Rosenzweig et al. 2007). Some of these studies have provided evidence that the
96 design of building storm-water drainage systems may be inadequate or at least under
97 designed for future climate conditions.

98 The purpose of this study is the assessment of possible changes in the *IDF* curves and
99 consequent designing of building storm-water drainage systems as a result of changes in
100 the distribution of extreme values of precipitation intensity due to the projected climate
101 change for Continental Portugal. Section 2 deals with description of the data and the
102 methodology used in this study. Results are presented and discussed in section 3.
103 Finally, section 4 is devoted to the conclusions.

104

105 **Material and Methods**

106 **Database / Data analysis**

107 In this work, the characterization of intense precipitation was substantiated with three
108 distinct databases. The first database consist of hourly precipitation time series obtained
109 from the database of the *Sistema Nacional de Informação e Recursos Hídricos*
110 [National System of Water Information and Resources] (SNIRH) for previously

111 selected weather stations, with the purpose of being representative of the three rainfall
112 areas defined in Matos and Silva (1986), (Fig. 1) and present in the Portuguese
113 Regulation-decree n.º 23/95 of August 23 (DR 1995). The selection criteria were based
114 on longevity and quality the historical series of hourly precipitation values (Table 1).
115 Time series cover between 8.2 (Castelo Melhor) and 12 (Covilhã) consecutive years,
116 which corresponds to 72 000 and 93 000 records, and have less than 5% of missing
117 values, excepting for stations located in mountainous rainfall region C (Covilhã and
118 Pega) but even so, with the 2nd and 3rd largest number of observed values (92 860 and
119 84 430 records).

120 With the aim to characterize the spatial distribution of extreme daily precipitation over
121 Continental Portugal, a second database of observed daily rainfall used in this study:
122 The most recent 8.0 version of the E-OBS gridded dataset (0.25 degree regular lat-lon
123 grid), released in April 2013 by ECA&D (<http://www.ecad.eu>) project (Haylock et al.
124 2008).

125 Finally, the third database consists of precipitation data simulated by the COSMO-CLM
126 [COnsortium for Small-scale MOdelling and Climate Limited-area Modelling
127 Community] (Rockel et al. 2008) regional climate model (RCM). The simulations are
128 run with ECHAM5/MPI-OM1 boundary conditions for recent climate conditions (20C,
129 1961 – 2000) and for two SRES scenarios (Nakicenovic et al. 2000), A1B and B1
130 (2000 – 2100). The resolutions of the rainfall data is roughly 18 km (0.165° latitude)
131 and 6-hourly. For this study, data for the spatial sub-domain defined between 36.6° N –
132 42.4° N and 6.2° W – 9.8° W is considered as it encompasses Portugal and the nearby
133 areas. The COSMO-CLM model has demonstrated its capacity to model the weather
134 and climate conditions, particularly temperature and precipitation, in different regions of
135 Europe. Furthermore, it has been used in several climate change studies analysing

136 changes of precipitation over Europe (e.g., Haslinger et al. 2012; Kotlarski et al. 2012)
137 and specifically in Portugal (Costa et al. 2012).

138 Precipitation indices suggested by the joint project Commission for
139 Climatology/Climate Variability and Predictability (CLIVAR)/Joint WMO/IOC
140 Technical Commission for Oceanography and Marine Meteorology Expert Team on
141 Climate Change Detection and Indices (Frich et al. 2002; Karl et al. 1999; Peterson
142 2005) are used to study climate change scenarios for precipitation extremes in Portugal
143 (cf. also Costa et al. 2012).

144

145 **Aggregation and disaggregation of precipitation**

146 The precipitation datasets described in the previous section are not available on time
147 scales adequate for this study. Consequently, it was necessary to use methods of
148 aggregation and disaggregation of precipitation, in order to have data of maximum
149 precipitation for the duration of 5 min, 10 min, 15 min, 30 min, 1 h, 2 h, 6 h, 12 h, 24 h
150 and 48 h. The aggregation process consisted on the use of precipitation depth values
151 obtained for smaller sampling durations to calculate precipitation depth values for
152 higher durations. For example, having hourly precipitation depth, it is rather easy to
153 obtain precipitation depth for 2, 6, 12, 24 and 48 h, simply by summing hourly values
154 that integrate the desired duration. This procedure was adopted for both databases
155 (observed and simulated), for higher durations than the sample ones. The disaggregation
156 of COSMO-CLM daily data to sub-daily data, namely, 1, 2, 6 and 12 h, was performed
157 using the method of fragments or coefficients of disaggregation of the maximum
158 precipitation values. Fragments (w_i) are the fraction of daily precipitation that occurred
159 at a given hour of the day (h_i),

$$w_i = \frac{h_i}{\sum_{i=1}^{24} h_i} \quad (2)$$

160

161 Consequently, the sum of the coefficients (w_i) for the 24 hours of the day is equal to the
 162 unit. Then, to estimate the precipitation depth in each hour of the day (h'_i), the
 163 corresponding fragment (w_i) is multiplied by the daily precipitation depth (d),

$$h'_i = w_i \times d \quad (3)$$

164

165 This disaggregation procedure assures that the hourly precipitation estimation (h'_i) does
 166 not change the total daily precipitation. The disaggregation fragments for 1, 2, 6 and
 167 12 hours were estimated from the hourly observed data by using the Equation (2).
 168 Fragments for each duration were computed and sorted in descending order, revealing
 169 that the arithmetic averages computed for 50, 100 and 200 highest values were very
 170 similar, and were adopted as the values of the coefficients of disaggregation, w_i . This
 171 disaggregation procedure assures that the adopted fragments allow an adequate
 172 estimation of the maximum precipitation depth for each duration while retaining
 173 consistency with the observed data. The adopted coefficients of disaggregation w_i were
 174 then applied to daily simulated data by the COSMO-CLM model using Equation (3) to
 175 estimate maximum precipitation depth for 1, 2, 6 and 12 hours for each cell of the
 176 model grid. This procedure was applied for to the recent and the future periods. The
 177 inexistence of observed precipitation data for sub-hourly sampling time compel the
 178 disaggregation precipitation process for these temporal scales to rely on the fragments
 179 obtained from the relationship between hourly and sub-hourly precipitation proposed
 180 for Portugal by Brandão et al. (2001). These disaggregation coefficients are in good
 181 agreement with those proposed in the Guide to Hydrological Practices of the World
 182 Meteorological Organization and studies performed by the Portuguese Meteorological
 183 Institute.

184

185 **Intensity-Duration-Frequency Curves**

186 The development of *IDF* curves that consider future climate conditions is critical for the
187 adequate design of building storm-water drainage systems, as it would allow mitigating
188 a possible change in the frequency and intensity of floods, and thus reducing the
189 damage associated with them. The methodology followed to develop the *IDF* curves is
190 equivalent to the estimation of the *a* and *b* parameters (Equation (1)), which includes
191 the: (i) computation of maximum precipitation intensity time series for each of ten
192 durations (5, 10, 15 and 30 min and 1, 2, 6, 12, 24 and 48 h); (ii) fitting of the Gumbel
193 distribution function to those time series, which mean estimate the location (μ) and
194 scale (σ) parameters in each case (cf. Coles 2001); (iii) estimation of precipitation
195 intensity for each duration and eight different return periods (2, 5, 10, 20, 50, 100, 500
196 and 1000 years) using Gumbel inverse distribution function; (iv) representation of the
197 precipitation intensity (mm/h) as a function of precipitation duration (min) in a log-log
198 plot to estimate the slope and intercept regression parameters. This last procedure
199 corresponds to linearization of the Intensity-Duration-Frequency curves (Equation (1)),

200

$$\log(I) = \log(a) + b \times \log(t) \quad (4)$$

201

202 which led to the estimation of the (*a* and *b*) *IDF* parameters with a statistical
203 significance level of 5%. The quality of the linear regression fit is also assessed by the
204 coefficient of determination (R^2), the *F-statistic* (*p - value*) and the error variance.

205 The adopted methodology is similar to that described in Brandão et al. (2001). The
206 major differences reside, on the one hand, on the way of adjusting the Gumbel law to

207 the data (likelihood estimation, using *evfit* function of MATLAB) and assessing the
208 quality of the fitting, made in this case with the Quantile-Quantile plots and
209 Kolmogorov-Smirnov test (*KStest*) and the use of robust regression method (RR) to
210 estimate the *IDF* parameters *a* and *b*. Major difference of RR in relation to the ordinary
211 least square method (OLS) used in Brandão et al. (2001) lies in the attribution of
212 weights to the observed points, as higher as the corresponding regression residual. A
213 deeper description of the RR method as well as the comparison with OLS may be found
214 in Holland et al. (1977), Huber (1981) and Street et al. (1988).

215 Many different methods can be used to derive *IDF* curves, from the usual univariate
216 empirical analysis of the intensity of rainfalls at fixed time intervals, to bivariate
217 frequency analysis using the copula method (Ariff et al. 2012), partial duration series
218 (Ben-Zvi 2009; Kingumbi and Mailhot 2010), multifractal approaches (Garcia-Marin et
219 al. 2013; Veneziano et al. 2013), ensemble empirical mode decomposition and scaling
220 properties (Bougadis and Adamowski 2006; Kuo et al. 2013). Several studies
221 comparing methodologies have been conducted but generally all methods seem to be
222 able to produce accurate *IDF* estimates (Mohyont et al. 2004; Veneziano et al. 2007;
223 Dame et al. 2008). The type I extreme value, (EVI or Gumbel) distribution has been
224 used successfully in many recent rainfall intensity studies in Europe (Llasat 2001; Bara
225 et al. 2010; Olsson et al. 2012), Asia (Ariff et al. 2012; Ben-Zvi 2009; Ahammed and
226 Hewa 2012), Africa (Kuo et al. 2013; Mohyont et al. 2004) and America (Lumbroso
227 et al 2011; Pizarro et al. 2012). EVI is currently the recommended distribution function
228 for use in Canada and the best choice for the estimation of *IDF* curves under changing
229 climate conditions (Das et al. 2013). Other distribution functions such as the general
230 extreme value type II (EVII or Fréchet) have also been used, e.g. to estimate the *IDF*
231 curves using short-record satellite data in Ghana (Endreny and Imbeah 2009).

232 The estimation of the *IDF* curves was performed for precipitation simulated by the
 233 ECHAM5/MPI-OM1 / COSMO-CLM model chain for the grid cells including the
 234 location of the six weather stations (cf. Table 1). With this aim, time series for 30 years
 235 period 1971 – 2000 for the C20 scenario, corresponding to the recent past weather
 236 conditions, and for two future climate scenarios SRES A1B and B1, regarding the
 237 periods 2011 – 2040, 2041 – 2070 and 2071 – 2100, were considered. In general,
 238 climate models are not capable of accurately reproduce the observed precipitation.
 239 Several methods can be used to correct this bias, ranging from the more traditional
 240 methods to the Delta Change approach, in order to include projected future changes in
 241 some key precipitation statistics (Olsson et al. 2012; Pereira et al. 2013). The procedure
 242 adopted here to correct the model bias is conditioned by just knowing the final values of
 243 the *IDF* parameters proposed in Matos and Silva (1986) and consisted of matching the
 244 values of the parameters obtained by the robust regression method for C20 (a_{C20} and
 245 b_{C20}) with the values (a_{MS} and b_{MS}) proposed by Matos and Silva (1986) which are the
 246 *IDF* parameters adopted by the Portuguese law (DR 1995). The correction factor of
 247 parameter a (Δa) results from the difference between the logarithm of parameter a_{C20}
 248 associated to scenario C20 and the logarithm of parameter a_{MS} from Matos and Silva
 249 (1986),

$$\Delta a = \log_{10} a_{C20} - \log_{10} a_{MS} \quad (5)$$

251
 252 In turn, the corrective factor of parameter b (Δb) results from the ratio between
 253 parameter b_{C20} associated to scenario C20 and parameter b_{MS} resulting from Matos and
 254 Silva's (1986) study,

$$\Delta b = \frac{b_{C20}}{b_{MS}}. \quad (6)$$

255

256 Afterwards, these same correction factors were applied to parameters a_{A1B} and b_{A1B}
257 obtained for scenario A1B, proceeding as follows:

258

$$a_{A1B\ corr} = 10^{(\log_{10} a_{A1B} - \Delta a)} \quad (7)$$

259

260 and

$$b_{A1B\ corr} = \frac{b_{A1B}}{\Delta b} \quad (8)$$

261

262 which allowed obtaining corrected versions of parameters a and b . The same procedure
263 was applied to intermediate results obtained for scenario B1.

264 The two-sample Kolmogorov-Smirnov test is used to compare the distributions of the
265 precipitation depth intensity simulated for future (I_{future}) and recent climate conditions
266 (I_{past}). The null hypothesis is that I_{future} and I_{past} are from the same continuous
267 distribution, while the alternative hypothesis is that they belong to different continuous
268 distributions. In both cases, the *IDF* curves ($I = a \times t^b$) are used to generate I values
269 for different duration times, by resorting to parameters estimated for future
270 periods/scenarios after correcting climate model bias and proposed by Matos and Silva
271 (1986), respectively.

272

273 **Design of the urban building drainage system**

274 The main goal of this study focuses on the comparison between the design of building
275 drainage systems, based on the *IDF* curves proposed in Matos and Silva (1986) and the
276 design based on *IDF* curves estimated for different periods of future scenarios for the
277 three rainfall regions (A, B and C, in Fig. 1). For quantitative comparison purpose and

278 sake of simplicity, specific residential roof drainage gutter and rainwater pipe were
279 considered as examples of building storm-water drainage systems to be designed. The
280 flows were calculated with the rational method equation,

281

$$Q = C.I.A \quad (9)$$

282

283 where, the contribution area (A) of the gutter is 100.14 m^2 , whereas the area of the
284 devices that reach the rainwater pipe is 155.69 m^2 , the flow coefficient (C) used for
285 building coverings is equal to the unit while the precipitation intensity (I) was
286 calculated according to the Equation (1) for a duration (t) of 5 minutes and a return
287 period (T) of 10 years. Parameters a and b used in the calculation of the precipitation
288 intensity follow the *IDF* curves established in the Regulation-decree n.º 23/95 (DR
289 1995), and those obtained for precipitation data simulated for future scenarios A1B and
290 B1, after correction of the climate model bias.

291 The gutter defined for conducting the storm water has a rectangular shape, with a base
292 (B) of 20 cm and inclination (i) of 0.5%. It was dimensioned so that the height of the
293 water depth (h) therein does not exceed $7/10$ of the total height of the gutter. The
294 Manning-Strickler's formula, Equation (10), was used with a roughness coefficient (K)
295 of $90 \text{ m}^{1/3}/\text{s}$, corresponding to metal plate. The hydraulic radius (R) and the area
296 occupied by the fluid (A_f), in the case of rectangular sections, are determined by the
297 Equation (11) and Equation (12), respectively:

$$Q = K \times A_f \times R^{2/3} \times i^{1/2} \quad (10)$$

$$R = \frac{B \times h}{(B + 2h)} \quad (11)$$

$$A_f = B \times h \quad (12)$$

298

299 The residential rainwater pipe was designed using the Manning-Strickler formula (10)
300 for full section, roughness (K) of $120 \text{ m}^{1/3}/\text{s}$ corresponding to polyvinyl chloride (PVC)
301 and inclination (i) of 2%. The hydraulic radius (R), in the case of a filled circular
302 section, is given by Equation (13), where D_i is the internal diameter of the piping.

$$R = \frac{D_i}{4} \quad (13)$$

303

304 **Results and discussion**

305 Before focussing in the *IDF* curves in three precipitation regions, we analyse the
306 precipitation distribution and projected changes for Continental Portugal. With this aim,
307 the long term (1961 – 2000) average of the annual maximum daily precipitation depth
308 was computed based on the ECAD precipitation dataset (Fig. 2). The obtained spatial
309 pattern is dominated by a region of very large values ($>60 \text{ mm}$), located over NW
310 Portugal. This pattern is quite different from the three rainfall areas configuration
311 proposed by Matos and Silva (1986) and adopted by the Portuguese legislator (Fig. 1).
312 Then, to assess potential future changes on extreme precipitation regime, four extreme
313 precipitation indices were computed using the precipitation dataset simulated by
314 COSMO-CLM for each of the 30-year periods for the C20, B1 and A1B scenarios,
315 namely: the total precipitation depth (*PRCTOT*); the long-term 95th percentile
316 (*PRC95p*); the ratio between *RR95pTOT* and *PRCTOT* (*R95T*); and, the total
317 precipitation depth falling in days with daily precipitation amounts greater than the
318 corresponding *PRC95p* (*RR95pTOT*). The computations were performed taking only
319 into account wet days defined as days with precipitation depth above or equal to 1.0
320 mm.

321 Results obtained for simulated recent–past climate conditions (C20 scenario, 1971 –
322 2000) over continental Portugal (Fig. 1) reveals high spatial variability in the total
323 precipitation depth, with values ranging between 11×10^4 mm in the NW part of the
324 country and 1×10^4 mm, in the remaining area of the country (Fig. 3(a)) resembling the
325 configuration of the average annual maximum daily precipitation depth (Fig. 2). This
326 spatial pattern is also very similar to the long term 95th percentile of the daily
327 precipitation depth (Fig. 3(b)), with highest values (as higher as 80 mm) located over
328 the NW quarter of country and in the southernmost region (of about 60 mm) and much
329 lower values (smaller than 45 mm) elsewhere.

330 The spatial distribution of *RR95pTOT* and *R95T* also helps to understand the regime of
331 extreme precipitation in Portugal. The spatial pattern of *RR95pTOT* (Fig. 3(c)) is very
332 similar to the *PRCTOT* but, as expected, with much lower values. This means that
333 precipitation amount falling in the days of extreme precipitation assume higher values
334 in the same regions where total precipitation depth is greater. The *R95T*, which is a
335 fraction (%) of total precipitation depth falling during extreme rainfall days, present a
336 pattern characterized by highest values (of about 30%) in the southern part of the
337 country and (of about 23%) on NW part of the country and along the Tagus river basin
338 (Fig. 3(d)).

339 Differences between the *PRC95p* ($\Delta PRC95p$) obtained for each of the 30-year period of
340 the future climate change SRES scenarios (B1 and A1B) and for the recent–past climate
341 conditions (C20 scenario) are displayed in Fig. 4. For the B1 scenario, positive
342 differences of 7 to 10 mm may be expected in the NW region with smaller magnitudes
343 elsewhere for the 2011-2040 period (Fig. 4(a)). The pattern for the following period
344 (2041 – 2070, Fig. 4(b)) is characterized by generally smaller values (< 5 mm) while for
345 the last 30-year period (2071 – 2100, Fig. 4(c)), resembles the 2011-2040 pattern except

346 in the southernmost area, where a decrease (of about -5 mm) in $PRC95p$ should be
347 expected. This is a clear indication that natural variability on longer time scales may be
348 superimposed on the long-term trends of precipitation associated with climate change.
349 For the A1B scenario and 2011 – 2040 period (Fig. 4(d)), a modest increase of the
350 $PRC95p$ is revealed in all territory, except in small and sparse regions in NW part of the
351 country. For latter periods (Fig. 4(e) and Fig. 4(f)), the pattern of the $\Delta PRC95p$ has the
352 same but amplified spatial configuration with values as high as +10 to 15 mm in the
353 NW region, over the Tagus river basin and southern part of the country for the 2071 –
354 2100 period.

355 Next, time series for the six weather stations are analysed. Given the ten temporal
356 durations, three 30-year periods (2011 – 2040, 2041 – 2070, and 2071 – 2100) for each
357 of the two future scenarios (A1B and B1) and one period for the recent past climate
358 conditions, a total of 420 time series is considered. The visual inspection of the
359 Quantile-Quantile plots and the value of the Kolmogorov-Smirnov statistical test (and
360 corresponding $p - value$) confirm the goodness of fit of the Gumbel distribution
361 function to all these time series. The probability density function for each scenario
362 suggests that the return period for a given amount of precipitation intensity decreases
363 for the three periods of the future scenarios vis-à-vis the period observed (not shown).

364 Values of the IDF parameters a and b used here were obtained by linear regression, for
365 durations times between 5 min and 30 min and return periods of 2, 5, 10, 20, 50 and 100
366 years. The quality of the regression was confirmed by the values of the coefficient of
367 determination (R^2), F -statistic and by the estimated error variance. The R^2 represents
368 fraction of the variance of the dependent variable (in this case, the precipitation intensity)
369 by the linear model using the independent variable (in this case the duration). In all
370 cases the values of R^2 were always higher than 0.99, which means that more than 99%

371 of the variance of intensity of precipitation can be explained by the variance of the
372 duration. The values of the *F-statistic* are used to assess the tests of nullity of
373 parameters for a given level of significance and it is reasonable to assume that the linear
374 regression equation fits the data well because of the high value of the *F-statistic* and the
375 *p – values* tends to zero for a significance level of 5%. Finally, the extremely small
376 value of the estimated error variance obtained in all cases supports the idea that the
377 regression line provides a good fit to the data.

378 The linear regression models based on the minimization of the squared error are based
379 on a number of assumptions which are not always verified, e.g. the non-normality of the
380 residuals, the existence of an asymmetric distribution of errors and outliers. This fosters
381 the use of the RR method in this study, which constitutes an alternative approach that
382 aims to be more robust and resistant than the OLS. Table 2 allows assessing changes in
383 the design of a residential gutter and rainwater pipe, as a consequence of variations
384 recorded in the *IDF* curves, as a result of the changes in the distribution of the
385 maximum precipitation values due to climate change. The determination of the design
386 flow was performed on the basis of the values of precipitation intensities estimated from
387 the *IDF* curves for all time periods and both scenarios (after bias correction) and *IDF*
388 curves currently used in designing building drainage systems in Portugal, developed by
389 Matos and Silva (1986) and embraced by the Portuguese legislation (DR 1995).

390 Overall, there is a clear tendency to increase the size of gutters and rainwater pipes
391 compared to the current dimensions defined in the Portuguese legislation (Table 2).
392 However, changes are not uniform: For region A, the estimated increases in the height
393 of the gutter for scenario A1B, range from 6% (2041 – 2070) to 11% (2071 – 2100) in
394 the station of Ponte da Barca, to 30% (2011 – 2040) to 39% (2071 – 2100) in São
395 Manços. For region B, the estimated increase may vary from 11% (2041 – 2070) to 39%

396 (2071 – 2100) for Castelo Melhor and scenario A1B and from 12% (2041 – 2070) to
397 28% (2071 – 2100) for scenario B1. In the station of Pinelo, the design of the gutter
398 varies from -7% (2011 – 2040) and 18% (2071 – 2100) for scenario A1B, whereas, for
399 scenario B1, it varies from 3% (2011 – 2040 and 2041 – 2070) and 10% (2071 – 2100).
400 In order to obtain an average value representative for the mid-21st century, averages
401 were built for each station over the three time periods, thus sampling decadal variability.
402 This results for example on an estimated average increase of 39% in São Manços and
403 9% for Ponte da Barca for the A1B scenario (both Region A). For region B, changes are
404 larger for Castelo Melhor (20%) than for Pinelo (5%) for both scenarios. On the
405 contrary, little differences are found for region C: ranges are 3% to 16% for scenario
406 A1B and from 3% to 9% for scenario B1 in the station of Covilhã, whereas for the
407 station of Pega, it ranges from 4% to 16% and from 3% to 6%, respectively.
408 Furthermore, averages were built over both stations in each region and both scenarios to
409 obtain values representative per region considering scenario uncertainty. Averaged
410 increase in Gutter dimension is likely to be higher in Region A (21%) than in region B
411 (12%) and in region C (7%).
412 The projected changes in the rainwater pipe size are essentially proportional to the
413 gutter (Table 2). Therefore, a detailed presentation of the results is omitted. The main
414 results are: (i) averaged changes in the rainwater pipe diameter increases from 4% in
415 region C, to 7% in region B and 11% in region A; (ii) different behaviour in region A is
416 characterized by higher changes in the weather stations located in the southern (São
417 Manços) than in the northern part (Ponte da Barca) and, in region B, at lower (Castelo
418 Melhor) than at higher altitude (Pinelo); (iii) higher homogeneity in the expected
419 changes in mountainous region C and (iv) changes are typically smaller than for the
420 gutter.

421 In general terms, the estimated changes are projected to be largest at the end of the 21st
422 century and under the conditions of scenario A1B scenario. In region C, there is a clear
423 increasing trend in the changes (increases) in the size of these building storm-water
424 drainage systems when the results for the three consecutive 30-year periods are
425 analysed, independently of the scenario considered. However, this behaviour is not
426 always observed in other regions where may even be expected decreasing trends (as in
427 São Manços, located in region A, for the conditions of scenario B1), probably
428 associated with natural variability on longer time scales. The temporal evolution of
429 patterns of the 95th percentile, allow the interpretation of the results obtained for the
430 expected changes in the dimensions of the rainwater collecting organs. In the case of the
431 A1B SRES scenario, the expected changes in the size of the gutter and rainwater pipe
432 along the three 30-year periods are characterized by increasing long-term trends in the
433 Pinelo, Pega and Covilhã stations; for São Manços and Castelo Melhor, changes of
434 similar magnitude are found for 2011 – 2040 and 2041 – 2070, which are enhanced for
435 2071 – 2100; For Ponte da Barca, a relative decrease is detected in the latter period at
436 least for the B1 scenario (Table 2). As mentioned above, part of these relative changes
437 between periods may be associated with multi-decadal natural climate variability and
438 not with a long-term climate trend. These projected changes are consistent with the
439 trends in the changes of *PRC95p* as discussed for the A1B scenario (Fig. 3).

440 Finally, it is important to underline that projected changes in the size of the building
441 storm-water drainage systems are statistical significant at the 99% level in all cases
442 except in the 6 cases (17%) identified by a dagger in Table 2 and for the station of Pega
443 in the first 30-year period of the A1B scenario. It is important to underline that
444 projected changes in all cases of rainfall region A are statistical significant (99%) and
445 that statistical significance is higher in the end of the XXI century.

446

447 **Conclusions**

448 This study aimed at discussing the current status of the *IDF* curves adopted by the
449 Portuguese Law and investigate the possible influence of projected changes in extreme
450 precipitation in the current designing of building storm-water drainage systems. Patterns
451 of spatial distribution of annual maximum daily rainfall and extreme precipitation
452 indices, obtained from both observed and simulated data for recent past conditions,
453 exhibit considerable variability and suggest the necessity to revise the results of Matos
454 and Silva (1986) included in the legislation (DR 1995), which divide Continental
455 Portugal in three homogeneous rainfall regions. This is the case even assuming the
456 long-term stationarity of current precipitation regime.

457 The developed methodology to assess the impacts of projected climate change is well
458 grounded in literature and ensures the robustness and statistical significance of the
459 results. The comparison of the design carried out with the *IDF* curves outlined for future
460 scenarios with the curves obtained by Portuguese law allowed estimating an average
461 increase of the gutter section and the rainwater pipe that is higher for region A (21% and
462 11%, respectively) than for region B (13% and 7%) and region C (7% and 4%).
463 Regarding the uncertainty for the three regions, estimated as the range between the two
464 stations, estimates were similar for region C, with maximum increases of 16% for the
465 gutter and 9% for the rainwater pipe. For region B, the estimates for gutter design varies
466 between 18% and 39% and, for the rainwater pipe range between 10% and 21%. For
467 region A, estimates are larger for southern Portugal (São Manços) – of 40% for the
468 gutter and 20% for the rainwater pipe – than for Northern Portugal (Ponte da Barca),
469 with 20% and 11% for the gutter and rainwater pipe, respectively. In spite of these
470 uncertainties, the sign of the trends are very consistent between regions and stations.

471 These tendencies are in line with the projected long-term changes of the 95th percentile
472 (*PRC95p*) and other extreme precipitation indices for under future climate conditions
473 which exhibit similar spatial patterns to the annual maximum daily rainfall. These
474 results, together with the spatial distribution of rainfall and extreme precipitation indices
475 seem to reinforce the suggested need to evaluate the precipitation regime classification
476 performed in Matos and Silva (1986).

477 Most cases studies discussed above (cf. Tab. 2) identified statistically significant
478 differences between the dimensions of the building storm-water drainage systems
479 estimated for recent and future climate conditions. This is also the case for the near-
480 future period of 2011 – 2041 and for the entire rainfall region A, which covers by far the
481 largest part of the mainland area.

482 In summary, the impact of projected climate change should be reflected in the overall
483 increase in the design of drainage storm-water drainage systems based on *IDF* curves as
484 defined in Portuguese law for all scenarios and future periods analysed. Projected
485 changes are typically larger and increasingly statistical significant for the end of the 21st
486 century, and the magnitude of the changes is larger for the scenario A1B than for
487 scenario B1. Current laws and regulations relating to the design and management of
488 hydraulic works may become out of date in the short term, given the increase in the
489 frequency and intensity of extreme precipitation events. Therefore, the design of new
490 building storm-water drainage systems for Continental Portugal should be modified to
491 larger dimensions to mitigate the projected changes in extreme precipitation

492

493 **Acknowledgements**

494 We thank the MPI for Meteorology (Germany), the WDCC/CERA database and the
495 COSMO-CLM community for providing the COSMO-CLM data. This work was

496 supported by European Union Funds (FEDER/COMPETE - Operational
497 Competitiveness Programme) and by Portuguese national funds (FCT - Portuguese
498 Foundation for Science and Technology) under the project FCOMP-01-0124-FEDER-
499 022692. We thank Sven Ulbrich (Univ. Cologne) for help with data handling, Sandra
500 Dias (UTAD), Fátima Ferreira (UTAD) and Cristina Costa (ISEGI) for discussions. We
501 acknowledge the E-OBS dataset from the EU-FP6 project ENSEMBLES
502 (<http://ensembles-eu.metoffice.com>) and the data providers in the ECA&D project
503 (<http://www.ecad.eu>).

504

505

506 **References**

- 507 Ahammed, F., Hewa, G. A. (2012). “Development of hydrological tools using extreme
508 rainfall events for Dhaka, Bangladesh.” *Water International* 37(1), 43-52.
509 DOI: 10.1080/02508060.2012.645191
- 510 Arganis-Juárez, M. L., Domínguez-Mora, R., Cisneros-Iturbe, H. L., Fuentes-Mariles,
511 G. E. (2008). “Génération d'échantillons synthétiques des volumes mensuels écoulés de
512 deux barrages utilisant la méthode de Svanidze modifiée.” *Hydrolog. Sci. J.* 53, 130-
513 141. DOI: 10.1623/hysj.53.1.130
- 514 Ariff, N. M., Jemain, A. A., Ibrahim, K., Zin, W. Z. W. (2012). “IDF relationships using
515 bivariate copula for storm events in Peninsular Malaysia.” *Journal of Hydrology* 470,
516 158-171. DOI: 10.1016/j.jhydrol.2012.08.045
- 517 Bara, M., Gaal, L., Kohnova, S., Szolgay, J., Hlavcova, K. (2010). “On the use of the
518 simple scaling of heavy rainfall in a regional estimation of idf curves in slovakia.”
519 *Journal of Hydrology and Hydromechanics* 58(1), 49-63. DOI: 10.2478/v10098-010-
520 0006-0
- 521 Beijo, L. A., Muniz, J. A., Neto, P. C. (2005). “Tempo de retorno das precipitações
522 máximas em Lavras (MG) pela distribuição de valores extremos do tipo I.” *Ciência e*
523 *Agrotecnologia* 29, 657-667. DOI: 10.1590/S1413-7054200500030002
- 524 Ben-Zvi, A. (2009). “Rainfall intensity-duration-frequency relationships derived from
525 large partial duration series.” *Journal of Hydrology* 367(1-2), 104-114.
526 DOI: 10.1016/j.jhydrol.2009.01.007

527 Bougadis, J., Adamowski, K. (2006). “Scaling model of a rainfall intensity-duration-
528 frequency relationship.” *Hydrological Processes* 20(17), 3747-3757.
529 DOI: 10.1002/hyp.6386

530 Brandão, C., Rodrigues, R., Costa, J. P. (2001). “Análise de fenómenos extremos,
531 Precipitações intensas em Portugal Continental.”
532 <http://snirh.pt/snirh/download/relatorios/relatorio_prec_intensa.pdf> (Feb. 1, 2013).

533 Coles, S. (2001). “An Introduction to Statistical Modeling of Extreme Values.”
534 Springer, London, UK, 209 pp.

535 Costa, A. C., Santos, J. A., Pinto, J. G. (2012). “Climate change scenarios for
536 precipitation extremes in Portugal.” *Theor. Appl. Climatol.* 108, 217-234.
537 DOI: 10.1007/s00704-011-0528-3

538 Dame, R. d. C. F., Teixeira, C. F. A., Terra, V. S. S. (2008). “Comparison of different
539 methodologies to estimate intensity-duration-frequency curves for pelotas - rs, brazil.”
540 *Engenharia Agricola* 28(2), 245-255. DOI: 10.1590/S0100-69162008000200005

541 Das, S., Millington, N., Simonovic, S. P. (2013). “Distribution choice for the
542 assessment of design rainfall for the city of London (Ontario, Canada) under climate
543 change.” *Canadian Journal of Civil Engineering* 40(2), 121-129. DOI: 10.1139/cjce-
544 2011-0548

545 Diodato, N., Bellocchi, G., Romano, N., Chirico, G. B. (2011). “How the
546 aggressiveness of rainfalls in the Mediterranean lands is enhanced by climate change.”
547 *Climatic Change* 108, 591-599. DOI: 10.1007/s10584-011-0216-4

548 DR (1995). “Decreto Regulamentar nº 23/95 (Regulation-decree nº 23/95).” *Diário da*
549 *República*, 194/95(I-B). <<http://www.dre.pt>> (Feb. 1, 2013).

550 Endreny, T. A., Imbeah, N. (2009). “Generating robust rainfall intensity-duration-
551 frequency estimates with short-record satellite data.” *Journal of Hydrology* 371(1-4),
552 182-191. DOI: 10.1016/j.jhydrol.2009.03.027

553 Fowler, H. J., Kilsby, C. G. (2003). “Implications of changes in seasonal and annual
554 extreme rainfall.” *Geophysical Research Letters* 30, 1720-1723. DOI:
555 10.1029/2003GL017327

556 Frich, P., Alexander, L. V., Della-Marta, P., Gleason, B., Haylock, M., Klein Tank, A.
557 M. G., Peterson T. (2002). “Observed coherent changes in climatic extremes during the
558 second half of the twentieth century.” *Climate Research* 19, 193-212.
559 DOI:10.3354/cr019193

560 Garcia-Marin, A. P., Ayuso-Munoz, J. L., Jimenez-Hornero, F. J., Estevez, J. (2013).
561 “Selecting the best IDF model by using the multifractal approach.” *Hydrological*
562 *Processes* 27(3), 433-443. DOI: 10.1002/hyp.9272

563 Haslinger, K., Anders, I., Hofstätter, M. (2012). “Regional Climate Modelling over
564 complex terrain: an evaluation study of COSMO-CLM hindcast model runs for the
565 Greater Alpine Region.” *Climate Dynamics* 40, 511-529. DOI: 10.1007/s00382-012-
566 1452-7

567 Haylock, M. R., Hofstra, N., Klein Tank, A. M. G., Klok, E. J., Jones, P. D., New, M.
568 (2008). “A European daily high-resolution gridded dataset of surface temperature and
569 precipitation.” *J. Geophys. Res (Atmospheres)* 113, D20119. DOI:
570 10.1029/2008JD010201

571 He, J., Valeo, C., Chu, A., Neumann, N. F. (2011). "Stormwater quantity and quality
572 response to climate change using artificial neural networks." *Hydrological Processes*
573 25, 1298-1312. DOI: 10.1002/hyp.7904

574 Holland, P. W., Welsch, R. E. (1977). "Robust Regression Using Iteratively Reweighted
575 Least-Squares." *Communications in Statistics: Theory and Methods* A6, 813-827.
576 DOI: 10.1080/03610927708827533

577 Huber, P. J. (1981). "Robust Statistics." John Wiley & Sons New York, Hoboken, NJ,
578 USA.

579 IPCC (2012). "Managing the Risks of Extreme Events and Disasters to Advance
580 Climate Change Adaptation." A Special Report of Working Groups I and II of the
581 Intergovernmental Panel on Climate Change, Field, C. B., Barros, V., Stocker, T. F.,
582 Qin, D., Dokken, D. J., Ebi, K. L., Mastrandrea, M. D., Mach, K. J., Plattner, G.-K.,
583 Allen, S. K., Tignor, M., Midgley P. M., eds., Cambridge University Press, Cambridge,
584 UK, and New York, NY, USA, 582 pp.

585 Karl, T. R., Nicholls, N., Ghazi, A. (1999). "CLIVAR/GCOS/WMO workshop on
586 indices and indicators for climate extremes: workshop summary." *Climate Change* 42,
587 3-7. DOI: 10.1007/978-94-015-9265-9_2

588 Kingumbi, A., Mailhot, A. (2010). "Intensity-Duration-Frequency (IDF) curves:
589 comparison of annual maximum and partial duration estimators." *Hydrological Sciences*
590 *Journal-Journal Des Sciences Hydrologiques* 55(2), 162-176.
591 DOI: 10.1080/02626660903545995

592 Kotlarski, S., Bosshard, T., Lüthi, D., Pall, P., Schär, C. (2012). "Elevation gradients of
593 European climate change in the regional climate model COSMO-CLM." *Climatic*
594 *Change* 112, 189-215. DOI: 10.1007/s10584-011-0195-5

595 Kuo, C.-C., Gan, T. Y., Chan, S. (2013). "Regional Intensity-Duration-Frequency
596 Curves Derived from Ensemble Empirical Mode Decomposition and Scaling Property."
597 *Journal of Hydrologic Engineering* 18(1), 66-74. DOI: 10.1061/(ASCE)HE.1943-
598 5584.0000612

599 Llasat, M. C. (2001). "An objective classification of rainfall events on the basis of their
600 convective features: Application to rainfall intensity in the northeast of Spain."
601 *International Journal of Climatology* 21(11), 1385-1400. DOI: 10.1002/joc.692

602 Lumbroso, D. M., Boyce, S., Bast, H., Walmsley, N. (2011). "The challenges of
603 developing rainfall intensity-duration-frequency curves and national flood hazard maps
604 for the Caribbean." *Journal of Flood Risk Management* 4(1), 42-52.
605 DOI: 10.1111/j.1753-318X.2010.01088.x

606 Mailhot, A., Duchesne, S., Caya, D., Talbot, G. (2007). "Assessment of future change in
607 intensity-duration-frequency (IDF) curves for southern Quebec using the Canadian
608 regional climate model (CRCM)." *Journal of Hydrology* 347(1-2), 197-210. DOI:
609 10.1016/j.jhydrol.2007.09.019

610 Maraun, D., Wetterhall, F., Ireson, A. M., Chandler, R. E., Kendon, E. J., Widmann, M.,
611 Brienen, S., Rust, H. W., Sauter, T., Themeßl, M., Venema, V. K. C., Chun, K. P.,
612 Goodess, C. M., Jones, R. G., Onof, C., Vrac, M., Thiele-Eich, I. (2010). "Precipitation
613 downscaling under climate change: recent developments to bridge the gap between

614 dynamical models and the end user.” *Rev Geophys* 48, RG3003.
615 DOI:10.1029/2009RG000314

616 Matos, R., Silva, M. (1986). “Estudos de precipitação com aplicação no projeto de
617 sistemas de drenagem pluvial. Curvas Intensidade-Duração-Frequência da precipitação
618 em Portugal.” ITH24 LNEC, Lisbon, Portugal

619 Meehl, G.A., Stocker, T. F., Collins, W. D., Friedlingstein, P., Gaye, A. T., Gregory, J.
620 M., Kitoh, A., Knutti, R., Murphy, J. M., Noda, A., Raper, S. C. B., Watterson, I. G.,
621 Weaver, A. J., Zhao, Z.-C. (2007). “Global Climate Projections.” *Climate Change*
622 *2007: The Physical Science Basis. Contribution of Working Group I to the Fourth*
623 *Assessment Report of the Intergovernmental Panel on Climate Change*, Solomon, S.,
624 Qin, D., Manning, M., Chen, Z., Marquis, M., Averyt, K. B., Tignor, M., Miller, H. L.,
625 eds., Cambridge University Press, Cambridge, United Kingdom and New York, NY,
626 USA, 747-845

627 Mohymont, B., Demaree, G. R., Faka, D. N. (2004). “Establishment of IDF-curves for
628 precipitation in the tropical area of Central Africa - comparison of techniques and
629 results.” *Natural Hazards and Earth System Sciences* 4(3), 375-387.

630 Nakicenovic, N., Alcamo, J., Davis, G., de Vries, B., Fenhann, J., Gaffin, S., Gregory,
631 K., Grubler, A., Jung, T. Y., Kram, T., La Rovere, E. L., Michaelis, L., Mori, S., Morita,
632 T., Pepper, W., Pitcher, H. M., Price, L., Riahi, K., Roehrl, A., Rogner, H.-H.,
633 Sankovski, A., Schlesinger, M., Shukla, P., Smith, S. J., Swart, R., van Rooijen, S.,
634 Victor, N., Dadi, Z. (2000). “Special Report on Emissions Scenarios.” Cambridge
635 University Press, Cambridge, UK, 612 pp.

636 Nie, L., Lindholm, O., Lindholm, G., Syversen, E. (2009). “Impacts of climate change
637 on urban drainage systems – a case study in Fredrikstad, Norway.” *Urban Water*
638 *Journal* 6, 323-332. DOI: 10.1080/15730620802600924

639 Olsson, J., Gidhagen, L., Gameraith, V., Gruber, G., Hoppe, H., Kutschera, P. (2012).
640 “Downscaling of Short-Term Precipitation from Regional Climate Models for
641 Sustainable Urban Planning.” *Sustainability* 4(5), 866-887. DOI: 10.3390/su4050866

642 Peck, A., Prodanovic, P., Simonovic, S. P. (2012). “Rainfall Intensity Duration
643 Frequency Curves Under Climate Change: City of London, Ontario, Canada.” *Canadian*
644 *Water Resources Journal* 37(3), 177-189. DOI: 10.4296/cwrj2011-935

645 Pereira, M. G., Calado, T. J., DaCamara, C. C., Calheiros, T. (2013). “Effects of
646 regional climate change on rural fires in Portugal.” *Climate Research* 57(3), 187-200.
647 DOI: 10.3354/cr01176

648 Peterson, T. C. (2005). “Climate change indices.” WMO Bulletin 54, 83–86.

649 Pizarro, R., Valdes, R., Garcia-Chevesich, P., Vallejos, C., Sanguesa, C., Morales, C.,
650 Balocchi, F., Abarza, A., Fuentes, R. (2012). “Latitudinal analysis of rainfall intensity
651 and mean annual precipitation in Chile.” *Chilean Journal of Agricultural Research*
652 72(2), 252-261.

653 Pui, A., Sharma, A., Mehrotra, R., Sivakumara, B., Jeremiaha, E. (2012). “A
654 Comparison of Alternatives for Daily to Sub-Daily Rainfall Disaggregation.” *Journal of*
655 *Hydrology* 470-471, 138-157. DOI: <http://dx.doi.org/10.1016/j.jhydrol.2012.08.041>

656 Rockel, B., Will, A., Hense, A. (2008). “The Regional Climate Model COSMO-CLM
657 (CCLM).” *Meteorologische Zeitschrift* 17, 347-348. DOI: 10.1127/0941-2948/2008/030

658 Rosenberg, E. A., Keys, P. W., Booth, D. B., Hartley, D., Burkey, J., Steinemann, A. C.,
659 Lettenmaier, D. P. (2010). "Precipitation extremes and the impacts of climate change on
660 stormwater infrastructure in Washington State." *Climatic Change* 102, 319-349.
661 DOI: 10.1007/s10584-010-9847-0

662 Rosenzweig, C., Major, D. C., Demong, K., Stanton, C., Horton, R., Stults, M. (2007).
663 "Managing climate change risks in New York City's system: assessment and adaptation
664 planning." *Mitig Adapt Strat Glob Change* 12, 1391-1409. DOI: 10.1007/s11027-006-
665 9070-5

666 Sharif, M., Burn, D. (2007). "Improved K -nearest neighbor weather generating model."
667 *Journal of Hydrologic Engineering* 12, 42-51. DOI: 10.1061/(ASCE)1084-
668 0699(2007)12:1(42)

669 Street, J. O., Carroll, R. J., Ruppert, D. (1988). "A Note on Computing Robust
670 Regression Estimates via Iteratively Reweighted Least Squares." *The American*
671 *Statistician* 42, 152–154. DOI: 10.1080/00031305.1988.10475548

672 Svanidze, G. G. (1964). "Principles of Estimating River-Flow Regulation by the Monte
673 Carlo Method." Metsniereba Press, Tbilisi, USSR

674 Svanidze, G. G. (1980). "Mathematical Modeling of Hydrologic Series." Water
675 Resources Publications, Fort Collins, Colorado.

676 Taylor, L. L., Banwart, S. A., Valdes, P. J., Leake, J. R., Beerling, D. J. (2012).
677 "Evaluating the effects of terrestrial ecosystems, climate and carbon dioxide on
678 weathering over geological time: a global-scale process-based approach." *Phil. Trans.*
679 *R. Soc. B* 367(1588), 565-582. DOI: 10.1098/rstb.2011.0251

680 Vasiljevic, B., McBean, E., Gharabaghi, B. (2012). "Trends in rainfall intensity for
681 stormwater designs in Ontario." *Journal of Water and Climate Change* 3(1), 1-10. DOI:
682 10.2166/wcc.2012.125

683 Veneziano, D., Lepore, C., Langousis, A., Furcolo, P. (2007). "Marginal methods of
684 intensity-duration-frequency estimation in scaling and nonscaling rainfall." *Water*
685 *Resources Research* 43, W10418. DOI:10.1029/2007WR006040

686 Veneziano, D., Yoon, S. (2013). "Rainfall extremes, excesses, and intensity-duration-
687 frequency curves: A unified asymptotic framework and new nonasymptotic results
688 based on multifractal measures." *Water Resources Research* 49(7), 4320-4334.
689 DOI: 10.1002/wrcr.20352

690 Zhu, J. (2013). "Impact of Climate Change on Extreme Rainfall across the United
691 States." *Journal of Hydrologic Engineering* 18(10), 1301-1309. DOI:
692 10.1061/(ASCE)HE.1943-5584.0000725

693 Zhu, J., Forsee, W., Schumer, R., Gautam, M. (2013). "Future projections and
694 uncertainty assessment of extreme rainfall intensity in the United States from an
695 ensemble of climate models." *Climatic Change* 118(2), 469-485. DOI: 10.1007/s10584-
696 012-0639-6

697 Zhu, J., Stone, M. C., Forsee, W. (2012). "Analysis of potential impacts of climate
698 change on intensity-duration-frequency (IDF) relationships for six regions in the United
699 States." *Journal of Water and Climate Change* 3(3), 185-196. DOI:
700 10.2166/wcc.2012.045

701

Tables

702
703
704
705
706
707

Table 1 – Weather stations used in this study. Characterization includes the code, name, abbreviation, altitude (H), geographical coordinates (latitude, longitude), cover period (P) and percentage of hourly precipitation missing values (MV).

Code	Name	Altitude (m)	Latitude (° N)	Longitude (° W)
03G/02C	Ponte da Barca, PB	39	41.80	-8.42
23K/01UG	São Manços, SM	190	38.46	-7.75
07O/05UG	Castelo Melhor, CM	286	41.01	-7.06
04R/02G	Pinelo, PI	607	41.63	-6.55
12L/03G	Covilhã, CO	719	40.28	-7.51
11O/01G	Pega, PE	770	40.43	-7.14

708

Code	Name	Alt (m)	Lat (° N)	Lon (° W)	P	MV (%)
03G/02C	Ponte da Barca, PB	39	41.80	-8.42	01/2003-09/2012	4.9
23K/01UG	São Manços, SM	190	38.46	-7.75	02/2001-03/2012	1.1
07O/05UG	Castelo Melhor, CM	286	41.01	-7.06	10/2001-12/2009	0.0
04R/02G	Pinelo, PI	607	41.63	-6.55	02/2003-01/2012	3.8
12L/03G	Covilhã, CO	719	40.28	-7.51	05/1998-05/2010	11.8
11O/01G	Pega, PE	770	40.43	-7.14	10/2001-03/2012	8.6

709
710
711

712 Table 2 – Projected changes in the dimension of the drainage systems. Height of the Gutter (H) and
713 diameter of the rainwater Pipe (D) designed for weather stations located in the three pre-defined rainfall
714 regions, using the precipitation intensity estimated by Portuguese law (DR 1995) and with data simulated
715 by COSMO-CLM, for three periods of thirty years of the two future scenarios (A1B and B1) as well as
716 the relative differences between these dimensions (ΔH and ΔD). Projected changes are statistical
717 significant at 99% level except for the cases identified by superscript lowercase letter (^a). Arithmetic
718 averages of ΔH and ΔD for each weather station ($\overline{\Delta H}_w$ and $\overline{\Delta D}_w$) and region and scenario ($\overline{\Delta H}_s$ and $\overline{\Delta D}_s$)
719 are also shown. The former values are calculated over different periods to obtain an average value
720 representative for the mid-21st century, thus sampling decadal variability. The latter are derived to obtain
721 values representative for each region considering scenario uncertainty.

Station	Scenario	Period	Gutter				Rainwater pipe			
			H (cm)	ΔH (%)	$\overline{\Delta H}_s$ (%)	$\overline{\Delta H}_w$ (%)	D (cm)	ΔD (%)	$\overline{\Delta D}_s$ (%)	$\overline{\Delta D}_w$ (%)
Region A	Ponte da Barca	DR n°23/95	4.51				96.60			
		A1B	2011-2040	4.92	9%	9%	101.48	5%	5%	11%
			2041-2070	4.79	6%		99.94	3%		
			2071-2100	5.01	11%		102.57	6%		
		B1	2011-2040	5.28	17%	17%	105.50	9%	9%	
			2041-2070	5.39	20%		106.81	11%		
	2071-2100		5.14	14%	103.90		8%			
	São Manços	DRn°23/95	4.51			21%	96.60			
		A1B	2011-2040	5.84	30%	33%	111.67	16%	17%	
			2041-2070	5.91	31%		112.38	16%		
			2071-2100	6.26	39%		116.00	20%		
		B1	2011-2040	6.17	37%	26%	115.06	19%	14%	
2041-2070			5.61	24%	109.13		13%			
2071-2100	5.28		17%	105.57	9%					
Region B	Castelo Melhor	DRn°23/95	3.89				88.80			
		A1B	2011-2040	4.50	16%	22%	96.52	9%	12%	7%
			2041-2070	4.33	11%		94.34	6%		
			2071-2100	5.41	39%		107.04	21%		
		B1	2011-2040	4.47	15%	18%	96.18	8%	10%	
			2041-2070	4.36	12%		94.76	7%		
	2071-2100		4.99	28%	102.31		15%			
	Pinelo	DRn°23/95	3.89			12%	88.80			
		A1B	2011-2040	3.63	-7%	4%	85.34	-4%	2%	
			2041-2070 ^a	3.91	1%		89.01	0%		
			2071-2100	4.57	18%		97.38	10%		
		B1	2011-2040 ^a	4.01	3%	5%	90.38	2%	3%	
2041-2070 ^a			4.00	3%	90.26		2%			
2071-2100	4.27		10%	93.74	6%					
Region C	Covilhã	DRn°23/95	5.09				103.44			
		A1B	2011-2040 ^a	5.25	3%	8%	105.22	2%	4%	4%
			2041-2070	5.37	5%		106.58	3%		
			2071-2100	5.89	16%		112.09	8%		
		B1	2011-2040	5.38	6%	6%	106.68	3%	3%	
			2041-2070	5.53	9%		108.32	5%		
	2071-2100 ^a		5.24	3%	105.03		2%			
	Pega	DRn°23/95	5.09			7%	103.44			
		A1B	2011-2040 ^b	5.29	4%	9%	105.64	2%	5%	
			2041-2070	5.45	7%		107.48	4%		
			2071-2100	5.93	16%		112.53	9%		
		B1	2011-2040 ^a	5.24	3%	5%	105.09	2%	3%	
2041-2070			5.39	6%	106.76		3%			
2071-2100	5.38		6%	106.63	3%					

722 ^a change is not statistically significant (p-values>0.05).

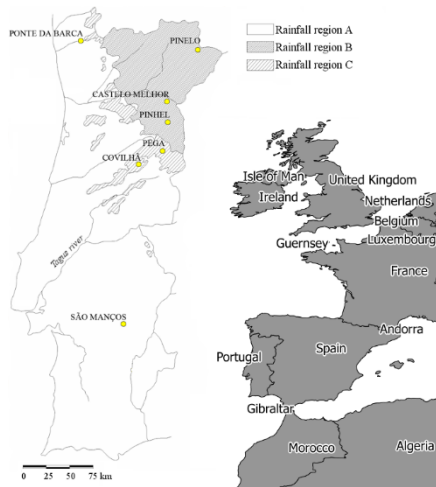
723 ^b change is statistically significant at 95% level

Figures

724

725

726



727

728

729

730

731

732

733

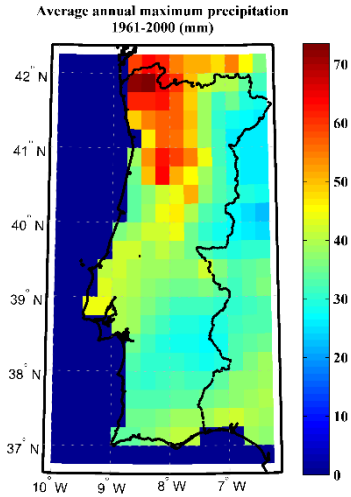
734

735

736

737

Figure 1 – Rainfall regions defined in the Portuguese Law (DR 1995), including the geographical location of the weather stations used in this study (left panel) and the geographical location of Continental Portugal in Western Europe (right panel).



738

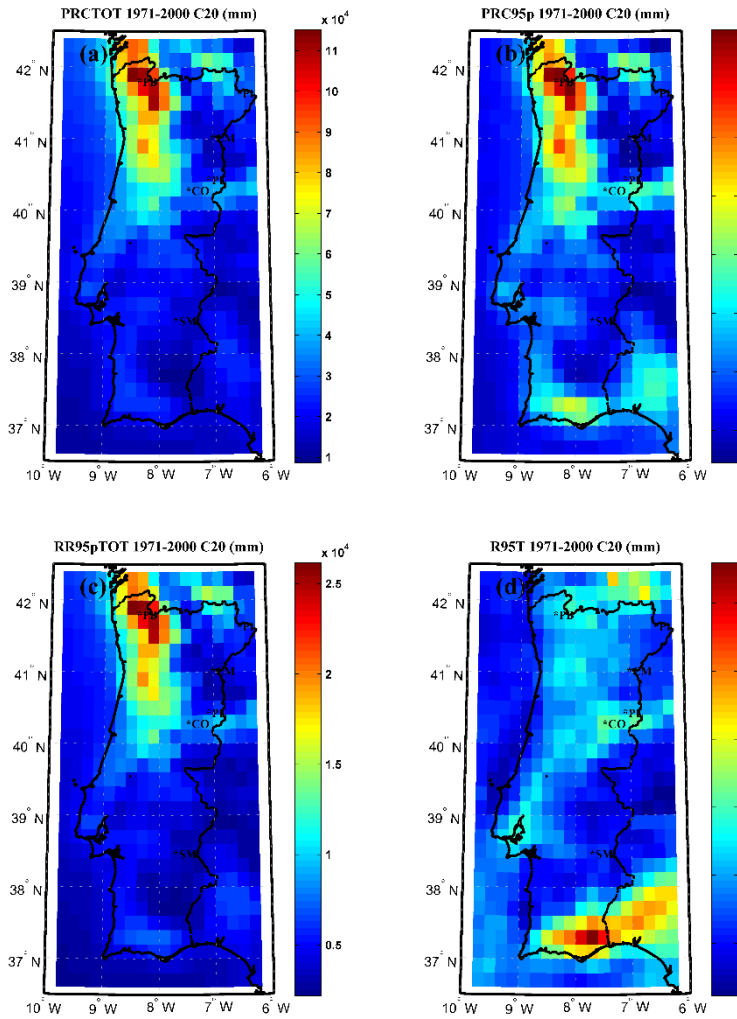
739

740

741

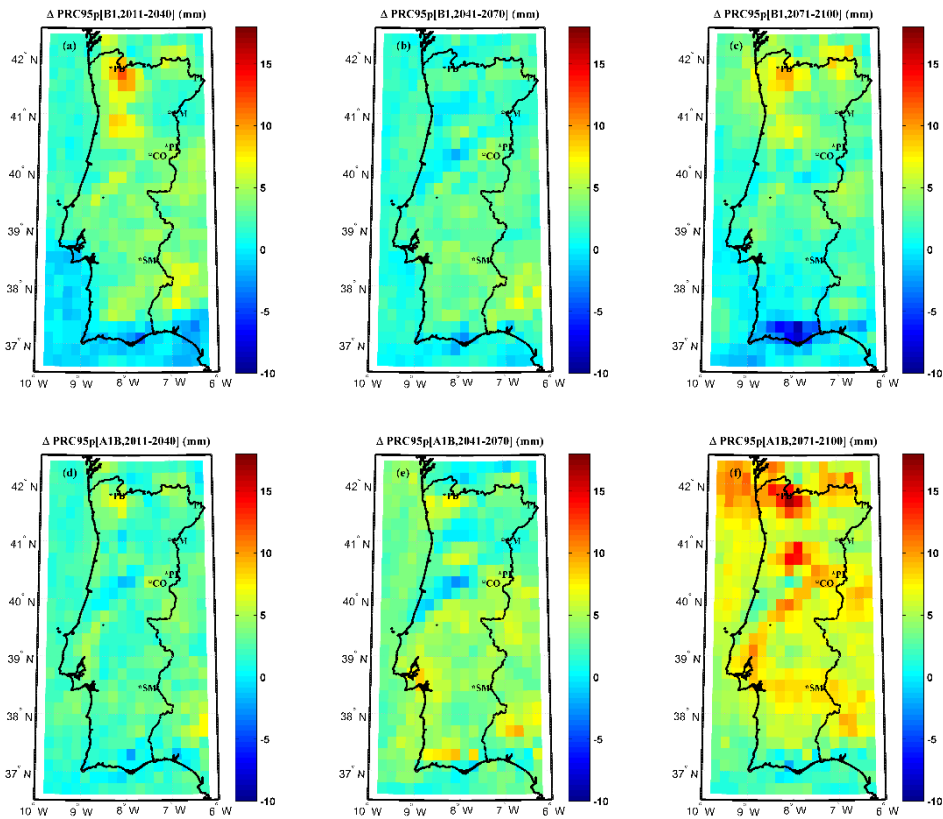
742

Figure 2 – The long-term (1961-2000) arithmetic average of the annual maximum daily precipitation. Values were evaluated with ECAD precipitation dataset (E-OBS v8.0, 0.25 degree regular lat-lon grid) over Continental Portugal.



743

744
 745 Figure 3 – Extreme Precipitation indices for Continental Portugal. Values of the (a) long-term 95th
 746 percentile (*PRC95p*), (b) total precipitation (*PRCTOT*), (c) total precipitation falling in days with daily
 747 precipitation amounts greater than the corresponding *PRC95p* (*RR95pTOT*) and (d) the ratio between
 748 *RR95pTOT* and *PRCPTOT* (*R95T*) evaluated for daily precipitation simulated by the COSMO-CLM
 749 model, for recent–past climate conditions (C20 scenario, 1971 – 2000).
 750



751

752

753

754

755

756

757

758

Figure 4 – Trends in long-term 95th percentile $PRC95p$ over continental Portugal. Differences between of the long-term 95th percentile ($\Delta PRC95p$) evaluated for future climate conditions under the B1 (top panel) and A1B (bottom panel) SRES scenarios and three 30-year periods 2011 – 2040 (left panels), 2041 – 2070 (middle panels) and 2071 – 2100 (right panels) in relation to recent–past climate conditions (C20 scenario, 1971 – 2000).